Bioorganic & Medicinal Chemistry Letters 21 (2011) 3411–3416

Contents lists available at ScienceDirect

Bioorganic & Medicinal Chemistry Letters

journal homepage: www.elsevier.com/locate/bmcl

# Macrocyclic lactams as potent Hsp90 inhibitors with excellent tumor exposure and extended biomarker activity

Christoph W. Zapf[a,*], Jonathan D. Bloom[a], Jamie L. McBean[a], Russell G. Dushin[a], Thomas Nittoli[a], Mercy Otteng[a], Charles Ingalls[a], Jennifer M. Golas[b], Hao Liu[b], Judy Lucas[b], Frank Boschelli[b], Yongbo Hu[c], Erik Vogan[d], Jeremy I. Levin[a]

[a] Medicinal Chemistry, 401 N Middletown Road, Pearl River, NY 10965, United States
[b] Oncology Research, 401 N Middletown Road, Pearl River, NY 10965, United States
[c] Structural Biology Computational Chemistry, Pfizer, 401 N Middletown Road, Pearl River, NY 10965, United States
[d] Structural Biology Computational Chemistry, Pfizer, 200 Cambridge Park Drive, Cambridge, MA 02139, United States

ARTICLE INFO

*Article history:*
Received 3 March 2011
Revised 25 March 2011
Accepted 29 March 2011
Available online 5 April 2011

*Keywords:*
Hsp90 inhibitors
Ortho-aminobenzamides
Tumor exposure
Macrocycles
Buchwald–Hartwig cyclization

ABSTRACT

A novel series of macrocyclic ortho-aminobenzamide Hsp90 inhibitors is reported. In continuation of our research in this area, macrocyclic amides and lactams were explored to reduce the risk of hERG liabilities. This effort culminated in the discovery of compound **38**, which showed a favorable in vitro profile, and efficiently suppressed proliferation of several relevant cell lines. This compound showed prolonged Hsp90-inhibitory activity at least 24 h post-administration, consistent with elevated and prolonged exposure in the tumor.

© 2011 Elsevier Ltd. All rights reserved.

Modern cancer chemotherapy generally suffers from the emergence of drug resistance.[1,2] The selective silencing of a specific cell signaling pathway by a chemotherapeutic is arguably at the origin of this problem. By up-regulating alternative pathways, tumors are able to adapt to the drug treatment and continue their growth. Targeting chaperone proteins offers a promising solution to this traditional chemotherapy dilemma, since it allows the simultaneous inhibition of multiple pathways with a single agent.[3,4]

The ATP-dependent 90 kDa molecular chaperone Hsp90 has become an attractive target for cancer therapy.[5,6] It plays a critical role in maintaining the function of a wide range of client proteins, many of which are intimately involved in cancer pathology.[7] Inhibition of Hsp90 leads to the destabilization, and ultimately the degradation of the clients, which results in the inhibition of cell growth and apoptosis.[8]

Different ATP-competitive chemotypes have evolved as potent N-terminal Hsp90 inhibitors, several of which have transitioned into clinical trials.[9–11] While many of these clinical trials focus on Hsp90 inhibitors as single agents for cancer therapy, combination studies with established chemotherapeutics have been designed and were reported recently as well.[12]

The first Hsp90 inhibitor reported in the literature was the macrocyclic natural product Geldanamycin **1** (Fig. 1), which belongs to the class of the ansamycins.[13] Clinical studies established this compound's unacceptable toxicology profile, preventing it from further development.[14] Optimization studies led to the discovery of 17-AAG **2** and 17-DMAG **3**[15] which are currently in clinical trials, but are characterized by poor solubility and a narrow therapeutic window, respectively.

Vernalis recently disclosed resorcinol **4**[16] which entered clinical trials in 2007. Isoxazole **4** is one of many small molecules which have been described in the literature as potential novel Hsp90 inhibitors with clinical application and is part of a recent summary on this topic.[17]

Serenex recently disclosed their own efforts to discover potent small-molecule Hsp90 inhibitors that would be devoid of the drawbacks associated with Geldanamycin.[18] Their studies culminated in a series of 2-aminobenzamides which exhibited low-nanomolar potencies in a proliferation assay. Among the reported compounds, glycine pro-drug SNX-5422 **5** was forwarded to clinical trials.[19]

In continuation of seeking potent small molecule inhibitors of Hsp90, and guided by X-ray crystallography using a structural analog of **5**, we were able to design and synthesize macrocyclic ortho-aminobenzamides. We recently disclosed a new series of

* Corresponding author. Tel.: +1 617 665 5602; fax: +1 617 665 5682.
*E-mail addresses:* chzapf@gmail.com, christoph.zapf@pfizer.com (C.W. Zapf).

0960-894X/$ - see front matter © 2011 Elsevier Ltd. All rights reserved.
doi:10.1016/j.bmcl.2011.03.112

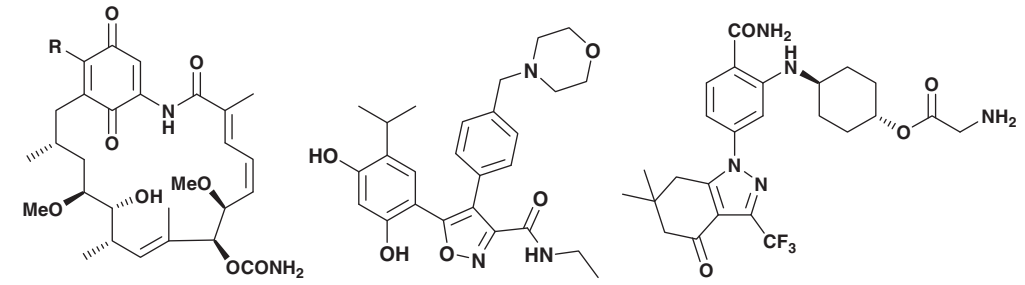


**Figure 1.** Structure of Geldanamycin **1**, clinically relevant ansamycins 17-AAG **2**, 17-DMAG **3**, Vernalis' clinical candidate NVP-AUY922 **4** and Serenex' clinical candidate SNX-5422 **5**.

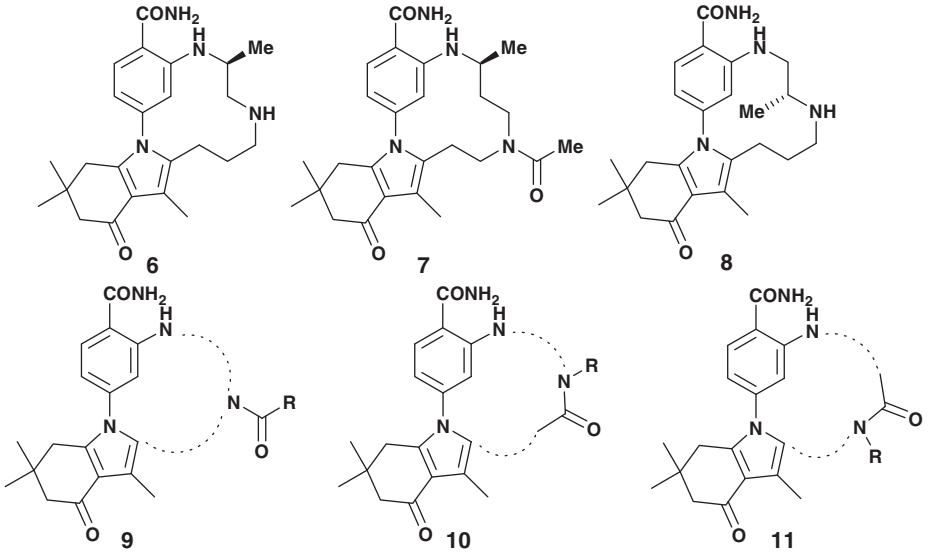


**Figure 2.** Previously reported macrocycles[20] and structures **8**–**11** discussed below.

macrocycles several of which are potent inhibitors of Hsp90 in an enzyme and a HCT116 cell-proliferation assay.[20] Beside its potency, analog **6** (Fig. 2) has acceptable solubility and rat microsomal stability. Compound **7**, which is devoid of the basic amine functionality, was found to be similarly potent but displayed poor stability in rat microsomes. Further investigations into the composition of the macrocyclic linker led to the discovery of amine **8** which is potent in the enzyme and cell-based assays (Table 1). Unfortunately, but not surprisingly, with its basic amine the compound is a potent inhibitor of the hERG ion channel ($IC_{50}$ = 3.2 μM).[21] This manuscript details a series of macrocyclic amides **9** and lactams **10**–**11** (Fig. 2) which were designed to mitigate hERG activity.

Previously reported macrocyclic amine **6** was elaborated to produce the exocyclic amides **12**–**17** (Scheme 1). Likewise, analogs **18**–**21** were obtained from the corresponding amine through standard amide formation chemistry.

The synthesis of a series of lactams is depicted in Scheme 2. The allyl-substituted tetrahydroindolone derivative **22** was advanced to the carboxylic acid derivative **24** following dihydroxylation, diol cleavage and oxidation under standard conditions. Amide formation utilizing different readily prepared Boc-protected amines **25** and subsequent deprotection, followed by Buchwald cyclization and hydrolysis yielded the desired target macrocycles **27**–**33**.

Employing similar chemistry, a related series of analogs was prepared in which the amide had been moved within the tether (Scheme 3). The respective amines **36** were accessed from the homo-allyl tetrahydroindolone **34** through the same sequence of dihydroxylation and cleavage followed by appropriate conversion to the desired primary or secondary amines as indicated. Acylations using the required protected alanine or (*S*)-homo-alanine was again followed by deprotection, cyclization and hydrolysis to produce analogs **38**–**43**.

Macrocycle **6**, reported previously, is a potent inhibitor of Hsp90 enzyme in the fluorescence-polarization binding assay[22], a cell-based vSrc assay[23] and a cell proliferation assay (Table 1). Related analog **8** is even more potent in all three assays but also a potent hERG inhibitor ($IC_{50}$ = 3.2 μM). We therefore sought macrocycles devoid of hERG activity. Analog **7** was used as a starting point since the hERG activity was attributed to the presence of the basic amine. Analog **7** was not quite as potent as **8**, which led to the design and preparation of amides **12**–**17**. While the enzyme potency suffered only slightly, the compounds behaved poorly in the cell-based assays. However, rat microsomal stability and solubility in most cases remained in the desired range.

**Table 1**
Biological activities, profiling data, and selected calculated properties for macrocycles **6**–**43**. For experimental details regarding assay conditions see ref.[22]

| # | Hsp90[a] | vSrc[b] | HCT116[c] | Rat[d] | Sol.[e] | MW[f] | TPSA[g] | *c*log*P*[h] |
|---|---|---|---|---|---|---|---|---|
| **6** | 0.11 | 0.116 | 0.093 | >30 | >100 | 409 | 89 | 4.1 |
| **7** | 0.111 | 0.108 | 0.151 | 9 | 19 | 451 | 97 | 2.8 |
| **8** | 0.091 | 0.047 | 0.043 | >30 | >100 | 409 | 89 | 4.1 |
| **12** | 0.09 | 0.917 | 1.009 | NT | NT | 466 | 123 | 2.6 |
| **13** | 0.2 | 6.183 | 4.894 | >30 | >100 | 480 | 123 | 2.8 |
| **14** | 0.119 | 0.488 | 0.71 | >30 | >100 | 480 | 123 | 2.9 |
| **15** | 0.145 | 0.238 | 0.314 | >30 | >100 | 480 | 123 | 2.9 |
| **16** | 0.14 | 0.674 | 1.55 | >30 | 5 | 508 | 127 | 2.6 |
| **17** | 0.14 | 0.109 | 0.168 | 3 | >100 | 494 | 101 | 3.6 |
| **18** | 0.219 | 0.111 | 0.194 | 11 | 69 | 451 | 97 | 3.4 |
| **19** | 0.953 | 1.159 | 1.897 | 12 | >100 | 451 | 97 | 3.4 |
| **20** | >5 | >5 | 3.263 | >30 | >100 | 494 | 101 | 4.1 |
| **21** | 0.555 | >5 | >5 | >30 | >100 | 480 | 123 | 3.5 |
| **27** | 6.831 | NT | NT | NT | NT | 409 | 106 | 1.9 |
| **28** | 0.214 | 0.522 | 0.815 | >30 | >100 | 423 | 106 | 2.5 |
| **29** | 0.156 | 0.16 | 0.247 | >30 | >100 | 437 | 97 | 2.9 |
| **30** | 0.608 | 0.278 | 0.865 | 12 | >100 | 465 | 97 | 3.7 |
| **31** | 0.222 | 0.108 | 0.359 | >30 | >100 | 481 | 107 | 3.4 |
| **32** | 0.191 | 0.249 | 0.33 | >30 | >100 | 494 | 101 | 3.5 |
| **33** | 0.407 | >5 | >5 | >30 | >100 | 508 | 127 | 2.4 |
| **38** | 0.082 | 0.079 | 0.056 | >30 | >100 | 423 | 106 | 3.5 |
| **39** | 0.268 | 0.123 | 0.175 | NT | NT | 423 | 106 | 3.5 |
| **40** | 0.092 | 0.06 | 0.08 | >30 | 34 | 437 | 97 | 3.9 |
| **41** | 1.181 | >20 | >20 | NT | >100 | 466 | 123 | 3.6 |
| **42** | 0.24 | 15.771 | 17.897 | >30 | >100 | 508 | 127 | 3.5 |
| **43** | 0.337 | 1.842 | 3.33 | NT | NT | 437 | 106 | 3.4 |

[a] Enzyme $IC_{50}$ [μM].
[b] Cell-based functional assay.
[c] Cell-proliferation $EC_{50}$ [μM].
[d] $t_{1/2}$ in rat microsomes [min].
[e] Solubility [μg/mL].
[f] Molecular weight.
[g] Total polar surface area;
[h] Calculated partition ratio.

We next decided to prepare acylated analogs of **6** and **8** which led to the synthesis of compounds **18**–**21**. While the physical properties of these compounds were mostly acceptable, their potency was generally reduced. This result was unexpected since this portion of the macrocyclic tether was thought to point toward the solvent exposed region of the enzyme.[20] However, molecular modeling suggested that the chemical nature of the tether can have a profound influence on the overall conformation of the macrocycle and thus on its biological activity.

Our next efforts focused on the preparation and evaluation of macrocyclic lactams **27**–**33**. The initial hypothesis was to test whether the amide itself would rigidify the unsubstituted tether sufficiently, rendering the stereocenter obsolete. However, a comparison of **27** and **28** quickly established that the incorporation of this methyl substitutent had again a dramatically positive effect on the potency of the macrocycle. Replacement of the amide NH with NMe (**29**) was beneficial, which led to the preparation of analogs **30**–**33**. Incorporation of larger amide substitutents, however, led to a reduction in potency.

Simultaneously to these efforts, the synthesis of lactams was carried out in which the amide group had been reversed and moved by one position along the tether toward the carboxamide. The first analog prepared in this series (**38**) is about equipotent to amine **8** in all three assays. This analog retains biological activity and physical properties while improving the calculated properties such as TPSA and *c*log*P*. Moreover, the compound shows only about a 7% inhibition of the hERG channel at 11 μM ($IC_{50}$ >33 μM), a substantial improvement over amine **8**, which inhibits hERG with 78% at the same concentration ($IC_{50}$ = 3.2 μM).[21] Inversion of the chirality (**39**) leads to a loss in potency while amide methylation (**40**) does not influence the excellent potency as expected when comparing **28** and **29**. Likewise, the incorporation of larger amide substituents (**41** and **42**) leads to an erosion of activity. To confirm our previous findings regarding ring-size, we prepared **43** in which the macrocycle is increased from a 12-membered to a 13-membered ring. As before, a consistent reduction in activity for this analog was observed.

The results in Table 1 showed consistent SAR trends and the cell-based vSrc data correlates well with the cell-proliferation data (Fig. 3). Activity was generally maintained or improved compared to the previously reported compounds[20] while rat microsomal stability and solubility were retained. These results prompted us to further characterize **38**.

An X-ray crystal structure of **40**, the *N*-methyl analog of **38**, bound to the N-terminal ATP-binding site of Hsp90 was obtained.[24] This substrate was chosen for the crystallographic studies since it contains an *N*-methyl substituent which was expected to provide

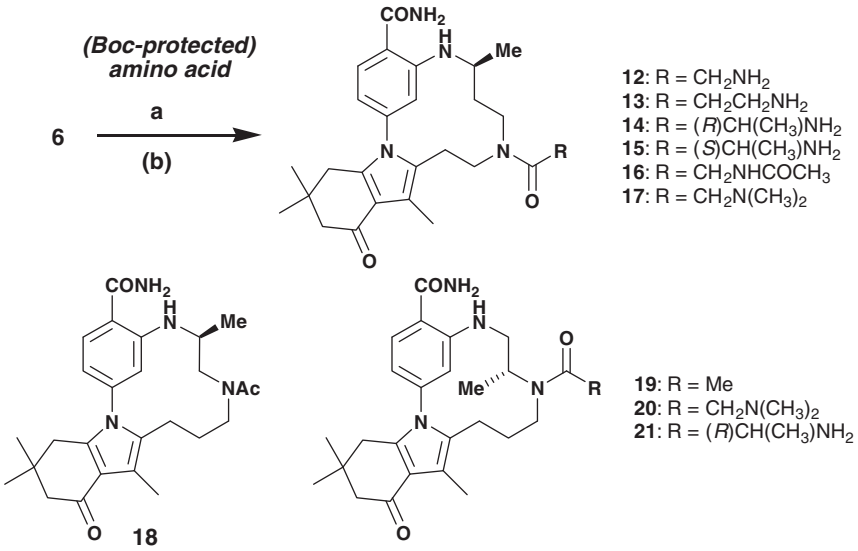


**Scheme 1.** Novel exocyclic amides **12**–**21**. (a) EDC, HOBt, $Et_3N$, DCM; (b) 10% TFA in DCM (if Boc-protecting group needed to be removed).

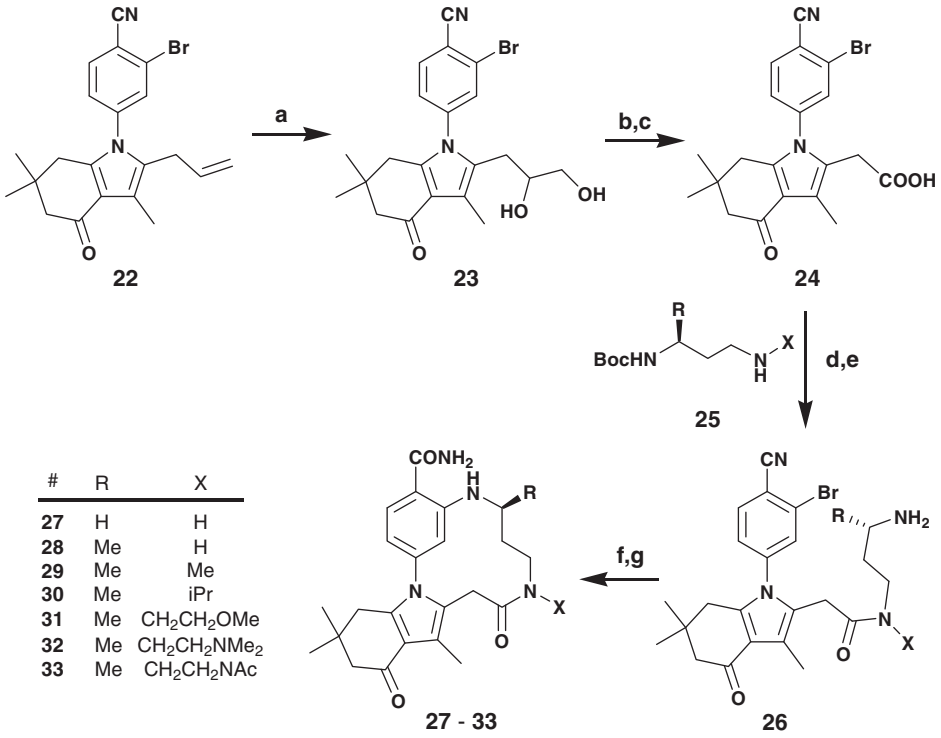


| # | R | X |
|---|---|---|
| **27** | H | H |
| **28** | Me | H |
| **29** | Me | Me |
| **30** | Me | iPr |
| **31** | Me | $CH_2CH_2OMe$ |
| **32** | Me | $CH_2CH_2NMe_2$ |
| **33** | Me | $CH_2CH_2NAc$ |

**Scheme 2.** (a) $OsO_4$, NMO, *t*BuOH, 70%; (b) $NaIO_4/SiO_2$, DCM, quant.; (c) $NaClO_2$, $NaH_2PO_4{\cdot}H_2O$, 2-methyl-2-butene, *tert*-BuOH, $H_2O$, 96%; (d) EDC, HOBt, $Et_3N$, DCM, 47–95%; (e) 10% TFA, DCM, quant.; (f) $Pd_2dba_3$, BINAP, NaO*t*Bu, dioxane, toluene, 110 °C, 45–98%; (g) 5 M NaOH, 30% $H_2O_2$, DMSO, EtOH, 44–78%.

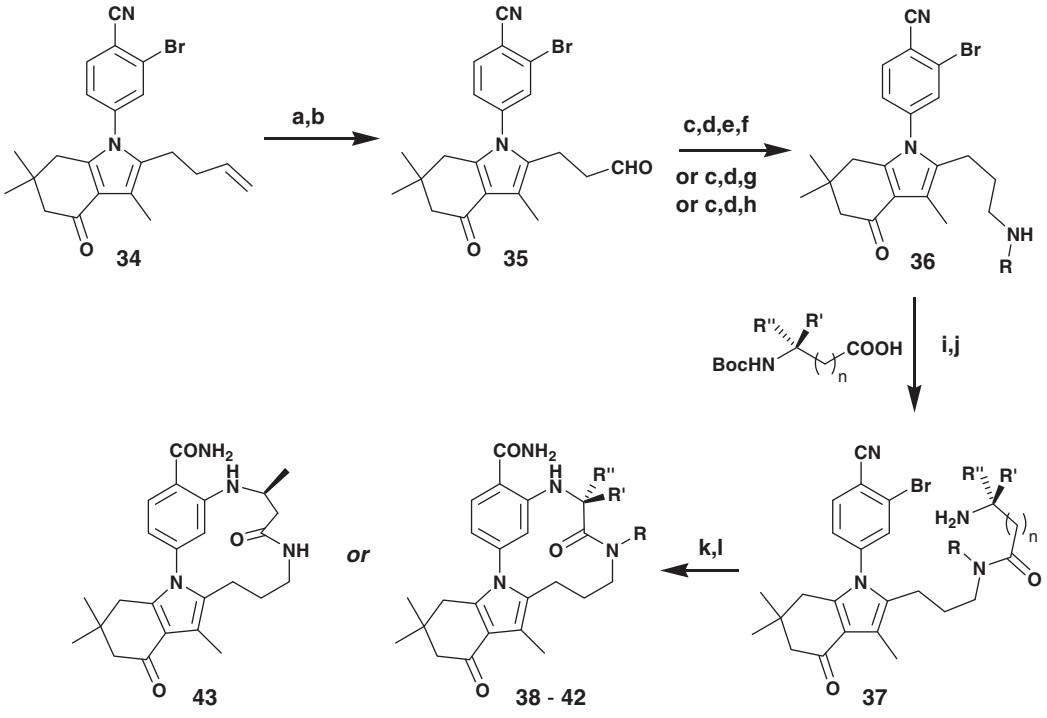


| # | R' | R'' | R |
|---|---|---|---|
| **38** | Me | H | H |
| **39** | H | Me | H |
| **40** | Me | H | Me |

| # | R' | R'' | R |
|---|---|---|---|
| **41** | Me | H | $(CH_2)_2NH_2$ |
| **42** | Me | H | $(CH_2)_2NHAc$ |

m

**Scheme 3.** (a) $OsO_4$, NMO, *t*BuOH, 70%; (b) $NaIO_4/SiO_2$, DCM, quant.; (c) $NaBH_4$, THF, 0 °C, 71%; (d) $MeSO_2Cl$, $Et_3N$, DCM; (e) $NaN_3$, DMF; (f) $PPh_3$, $H_2O$; (g) $MeNH_2$; (h) $BocNHCH_2CH_2NH_2$; (i) EDC, HOBt, $Et_3N$, DCM, 47–95%; (j) 10% TFA, DCM, quant.; (k) $Pd_2dba_3$, BINAP, NaO*t*Bu, dioxane, toluene, 110 °C; (l) 5 M NaOH, 30% $H_2O_2$, DMSO, EtOH; (m) $Ac_2O$.

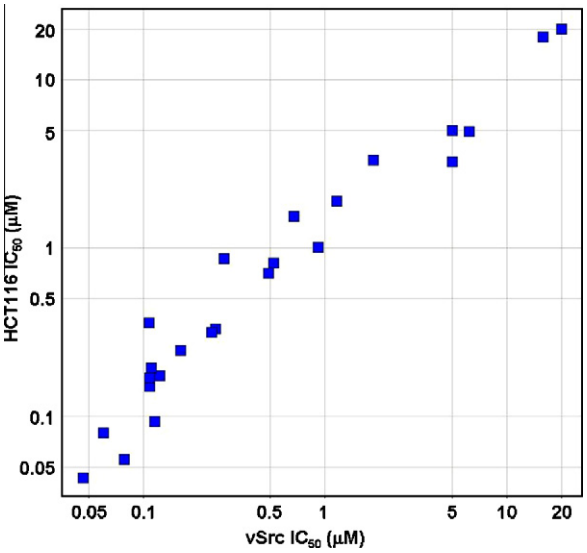


**Figure 3.** vSrc activity correlates with proliferation activity.

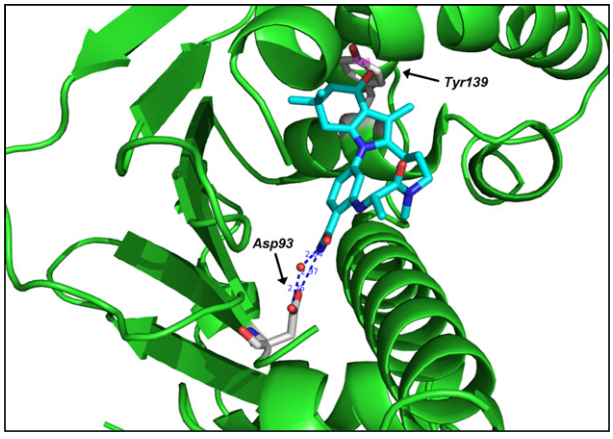


**Figure 4.** X-ray crystal structure of macrocycle **40** bound to the N-terminal Hsp90 binding site.

valuable SAR information. Its increased potency compared to analogs **41** and **42** was expected to contribute to an improved crystallization behavior. As can be seen in Figure 4, the carbonyl of the tetrahydroindolone engages in a hydrogen bond with Tyr139 while the benzamide interacts with Asp93 in a direct and a water-mediated hydrogen bond. The X-ray structure of **40** indicates that the methyl amide is pointed toward the protein in essence explaining the drop in activity for derivatives **41** and **42** with their bulkier substituents.

These macrocyclic o-aminobenzamides bind to the N-terminal ATP binding pocket of ATP (Fig. 4) and are as such competitive ATP inhibitors. However, a substantial conformational difference can be noted when comparing the binding conformation of ATP in the active site of Hsp90 with its conformation in kinases. Compound **38** was tested against the Invitrogen panel of 59 kinases and was found to inhibit these kinases with an $IC_{50}$>50 μM.

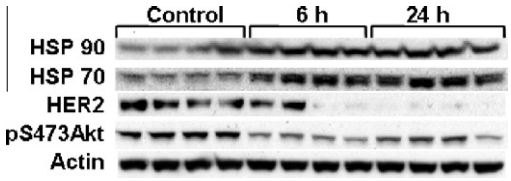


**Figure 5.** Biomarker effects of **38** at 50 mg/kg PO. Each vertical lane with its five markers represents data from an individual animal.

**Table 3**
Exposure levels of **38** after 50 mg/kg PO dosing

| | 6 h | 24 h |
|---|---|---|
| Plasma | 146 ng/mL | 8 ng/mL |
| Tumor | 2129 ng/g | 1266 ng/g |

Further characterization of **38** in other cell lines revealed a broad spectrum of remarkable activity across various cell lines including melanoma (A375, WM266-4), lung (A549, NCI-1975), breast (BT474, MDAMB361), prostate (DU145), colon (HCT116) and glioblastoma (T98G, U87MG) cells (Table 2). The compound also showed activity in KB cells and MDR cells (KB8.5) but was inactive in cells expressing high levels of P-gp transporters (KBV1).

We next studied **38** in a biomarker efficacy study in a xenograft model using MDA-MB-361 tumors (Fig. 5). When administered at 50 mg/kg PO, the compound clearly elicits a heat-shock response characterized by an up-regulation of Hsp90 and Hsp70. This effect can be seen 6 and even 24 h post dosing. It was hypothesized that this prolonged exposure could translate to an extended pharmacodynamic effect and ultimately to an improved dosing schedule in the clinic. Another characteristic response to effective Hsp90 inhibition is the down-regulation of HER2 a well-known substrate for this chaperone. Similarly, phosphorylated Akt is also down-regulated at the same time points.

Tissue and blood levels of **38** were also measured in this biomarker study. As can be seen in Table 3, rapid clearance of the compound was observed from the blood while the tumor levels remained high throughout the 24 h experiment consistent with the biomarker results.

In conclusion, we were able to optimize potent macrocyclic amine **8** with its hERG liability to an equipotent lactam devoid of ion channel activity while retaining excellent physical properties. The clear biomarker activity of lactam **38** even at 24 h post PO dosing and its high exposure levels in the tumor provides relevant SAR insight. Improved macrocyclic analogs with in vivo efficacy will be reported in due course.

**Table 2**
Effect of **38** on proliferation in various cell lines

| | | | | | | | |
|---|---|---|---|---|---|---|---|
| Cell line | A375 | WM266-4 | A549 | NCI-1975 | BT474 | MDAMB361 | DU145 |
| $IC_{50}$ [nM] | 23 | 92 | 23 | 47 | 23 | 111 | 45 |
| Cell line | HCT116 | T98G | U87MG | KB | KB8.5 | KBV1 | |
| $IC_{50}$ [nM] | 56 | 42 | 80 | 22 | 49 | >1000 | |

## References and notes


1. Borst, P.; Jonkers, J.; Rottenberg, S. *Cell Cycle* **2007**, *6*, 2782.
2. Nobili, S.; Landini, I.; Giglioni, B.; Mini, E. *Curr. Drug Targets* **2006**, *7*, 861.
3. Blagg, B. S.; Kerr, T. D. *Med. Res. Rev.* **2006**, *26*, 310.
4. Neckers, L. *J. Biosci.* **2007**, *32*, 517.
5. Isaacs, J. S.; Xu, W.; Neckers, L. *Cancer Cell* **2003**, *3*, 213.
6. Solit, D. B.; Chiosis, G. *Drug Discov. Today* **2008**, *13*, 38.
7. Whitesell, L.; Lindquist, S. L. *Nat. Rev. Cancer* **2005**, *5*, 761.
8. Maloney, A.; Workman, P. *Expert Opin. Biol. Ther.* **2002**, *2*, 3.
9. Taldone, T.; Sun, W.; Chiosis, G. *Bioorg. Med. Chem.* **2009**, *17*, 2225.
10. Messaoudi, S.; Peyrat, J. F.; Brion, J. D.; Alami, M. *Anticancer Agents Med. Chem.* **2008**, *8*, 761.
11. Drysdale, M. J.; Brough, P. A. *Curr. Top. Med. Chem.* **2008**, *8*, 859.
12. Hwang, M.; Moretti, L.; Lu, B. *Curr. Med. Chem.* **2009**, *16*, 3081.
13. Whitesell, L.; Mimnaugh, E. G.; De Costa, B.; Myers, C. E.; Neckers, L. M. *Proc. Natl. Acad. Sci. U.S.A.* **1994**, *91*, 8324.
14. Supko, J. G.; Hickman, R. L.; Grever, M. R.; Malspeis, L. *Cancer Chemother. Pharmacol.* **1995**, *36*, 305.
15. Tian, Z. Q.; Liu, Y.; Zhang, D.; Wang, Z.; Dong, S. D.; Carreras, C. W.; Zhou, Y.; Rastelli, G.; Santi, D. V.; Myles, D. C. *Bioorg. Med. Chem.* **2004**, *12*, 5317.
16. Brough, P. A.; Aherne, W.; Barril, X.; Borgognoni, J.; Boxall, K.; Cansfield, J. E.; Cheung, K. M.; Collins, I.; Davies, N. G.; Drysdale, M. J.; Dymock, B.; Eccles, S. A.; Finch, H.; Fink, A.; Hayes, A.; Howes, R.; Hubbard, R. E.; James, K.; Jordan, A. M.; Lockie, A.; Martins, V.; Massey, A.; Matthews, T. P.; McDonald, E.; Northfield, C. J.; Pearl, L. H.; Prodromou, C.; Ray, S.; Raynaud, F. I.; Roughley, S. D.; Sharp, S. Y.; Surgenor, A.; Walmsley, D. L.; Webb, P.; Wood, M.; Workman, P.; Wright, L. *J. Med Chem.* **2008**, *51*, 196.
17. Biamonte, M. A.; Van de Water, R.; Arndt, J. W.; Scannevin, R. H.; Perret, D.; Lee, W. C. *J. Med. Chem.* **2010**, *53*, 3.
18. Barta, T. E.; Veal, J. M.; Rice, J. W.; Partridge, J. M.; Fadden, R. P.; Ma, W.; Jenks, M.; Geng, L.; Hanson, G. J.; Huang, K. H.; Barabasz, A. F.; Foley, B. E.; Otto, J.; Hall, S. E. *Bioorg. Med. Chem. Lett.* **2008**, *18*, 3517.
19. Huang, K. H.; Veal, J. M.; Fadden, R. P.; Rice, J. W.; Eaves, J.; Strachan, J. P.; Barabasz, A. F.; Foley, B. E.; Barta, T. E.; Ma, W.; Silinski, M. A.; Hu, M.; Partridge, J. M.; Scott, A.; DuBois, L. G.; Freed, T.; Steed, P. M.; Ommen, A. J.; Smith, E. D.; Hughes, P. F.; Woodward, A. R.; Hanson, G. J.; McCall, W. S.; Markworth, C. J.; Hinkley, L.; Jenks, M.; Geng, L.; Lewis, M.; Otto, J.; Pronk, B.; Verleysen, K.; Hall, S. E. *J. Med. Chem.* **2009**, *52*, 4288.
20. Zapf, C. W.; Bloom, J. D.; McBean, J. L.; Dushin, R. G.; Nittoli, T.; Ingalls, C.; Southerland, A.; Sonye, J. P.; Eid, C. N.; Golas, J. M.; Liu, H.; Boschelli, F.; Vogan, E. M.; Hu, Y.; Levin, J. I. *Bioorg. Med. Chem. Lett.* **2011**, *21*, 2278.
21. $IC_{50}$s were obtained from a standard Ionworks HT patch clamp assay.
22. Gopalsamy, A.; Shi, M.; Golas, J.; Vogan, E.; Jacob, J.; Johnson, M.; Lee, F.; Nilakantan, R.; Petersen, R.; Svenson, K.; Chopra, R.; Tam, M. S.; Wen, Y.; Ellingboe, J.; Arndt, K.; Boschelli, F. *J. Med. Chem.* **2008**, *51*, 373.
23. Boschelli, F.; Golas, J. M.; Petersen, R.; Lau, V.; Chen, L.; Tkach, D.; Zhao, Q.; Fruhling, D. S.; Liu, H.; Nam, C.; Arndt, K. T. *Cell Stress Chaperones* **2010**, *15*, 913.
24. The structure has been assigned PDB ID code 3R91.